On infragravity waves and nearshore barred morphology

B.G. Ruessink

Abstract

Multiple bar systems often exhibit cyclic behaviour on the time scale of years. The role of infragravity waves in explaining this behaviour is investigated by reviewing the existing literature and by presenting observational evidence from field observations in 3 to 9 m depth. It appears that mechanisms involving standing long waves are unlikely to be of importance, as their predicted morphological behaviour contrasts strongly with our phenomenological knowledge of interannual bar behaviour. Field observations of sediment transport fluxes in the Terschelling bar system strongly suggest that wave asymmetry and undertow are the main small-scale processes driving morphological change. The role of infragravity waves seems to be of minor importance. The linkage of the small-scale processes to the observed interannual cyclic bar behaviour is at present only conceptual; however, it may serve as a first step towards a more coherent morphodynamic model capable of explaining cyclic bar behaviour.

205

1   Introduction

The analysis of a data set of annual soundings of the sandy Dutch nearshore zone, obtained since 1964 by the Dutch Public Works Department, has revealed the presence of 1 to 3 inter- and subtidal bars. The behaviour of these bars in time is interrelated and the bars can therefore be considered as a multiple bar system. On the time scale of years (herein referred to as the medium time scale) the bar behaviour has a cyclic nature (e.g., Ruessink and Kroon, 1994; Wijnberg and Terwindt, 1995). The former authors developed a 3-stage model to describe the cross-shore evolution of a bar through such a cycle. Their model consists of bar generation in the inner nearshore in water depths of 1 to 2 m (stage 1), net offshore bar migration through the surf zone to depths of about 4 to 6 m (stage 2) and bar decay in the outer nearshore zone in depths of 5 to 7 m (stage 3). The trigger of this cyclic behaviour seems to be the outer subtidal bar: its degeneration is followed by the onset of offshore migration of the inner bar and the formation of a new bar near the shoreline.
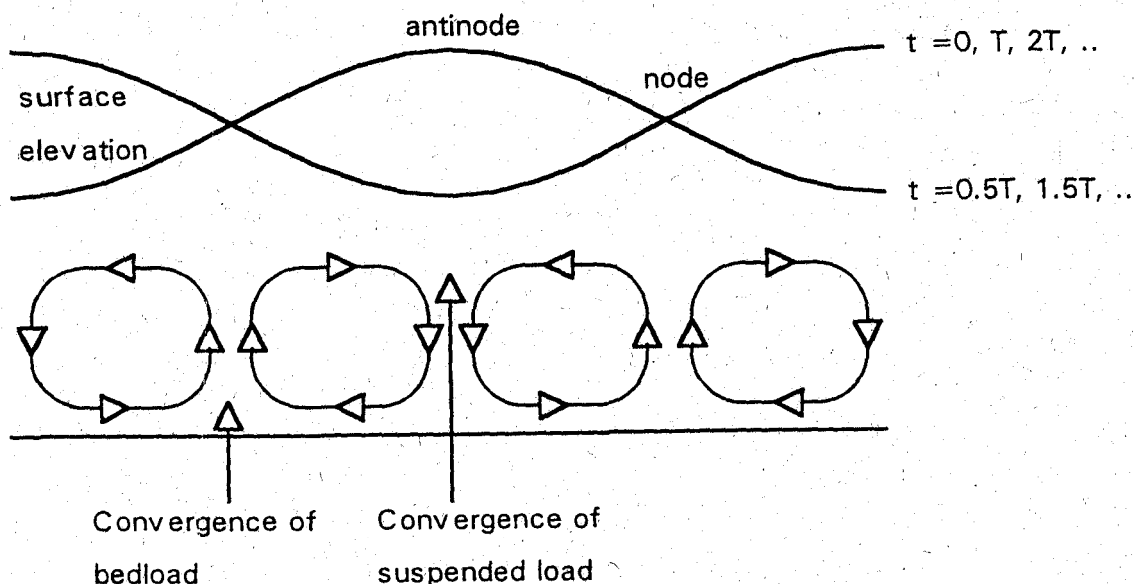
The net offshore migration is not a continuous phenomenon, but an intermittent process confined to high-energy periods. Similar cyclic, medium-scale offshore directed bar behaviour has been observed along other sandy coastlines under different boundary conditions (e.g., Lippmann et al., 1993; Shand and Bailay, 1998). The causes of this apparently rather common cyclic behaviour are, however, poorly understood.

The general approach to study coastal behaviour is to consider the coast as a geomorphic system. Such a system consists of several compartments, each having its own distinct spatial and temporal scale. For each compartment a morphodynamic system can be identified, in which water motion, sediment transport and morphology at corresponding scales interact. The water motion results from the energy input of wind, waves and currents, and is the driving force for sediment transport. Gradients in the sediment transport result in morphological change, which, in turn, influences the water motion. Infragravity waves, broadly defined as motions in the frequency range 0.004 - 0.04 Hz, are generally considered as the water motions that have the same spatial scale as nearshore bars (Bowen, 1980; Holman and Bowen, 1982; among many others).

Bar formation mechanisms involving infragravity waves can be divided into two groups based on whether the gradients in the sediment transport are induced by (1) the second-order drift velocities associated with standing infragravity waves, or (2) the primary orbital infragravity motions. At first glance, it may seem strange that the second-order motions are mentioned prior to the first-order motions. However, in this way the coupling between infragravity waves and nearshore bars is put into its historical perspective. The second class can be further subdivided into two additional types. In the first type (2a) infragravity waves are considered to be the only generative process responsible for morphological changes, whereas in the second type (2b) additional flows related to wave asymmetry and undertow are considered as well. It is the aim of the present paper to review the existing literature on the infragravity-bar mechanisms, to present new observational evidence and to discuss the pros and cons of the various mechanisms in light of the above mentioned phenomenological knowledge of medium-scale multiple-bar behaviour. It will be shown that the first ideas on infragravity waves and bars focussed entirely on the secondary drift velocities, but that they have been gradually replaced by the notion that the primary orbital motions of infragravity waves act together with other surfzone induced flows. The linkage of these flows to medium-scale bar behaviour is, however, still in its infancy.

Type 1: second-order infragravity motions

In case of full standing waves, a pattern of quarter-wavelength circulation cells develops in the bottom boundary layer (Figure 1; Carter et al., 1973). At the bottom of these cells the residual (i.e. second-order) flow (or drift) is directed towards the node of the surface elevations, while at the top the residual current

antinode

node

t =0, T, 2T, ..

surface
elevation

t =0.5T, 1.5T, ..

207

Convergence of
bedload

Convergence of
suspended load

Figure 1   Cells with residual flow under a standing wave with period T.

flows in the opposite direction. Consequently, if bed load prevails, sediment converges under the node of the surface elevation, whereas if suspended load is the dominant transport mechanism, bar formation is expected under the antinode. An important requirement in the standing-wave hypothesis is the dominance of a single infragravity frequency. A broad-banded spectrum of infragravity waves inhibits bar formation, as the contributions of all frequencies to the sediment transport cancel out (Holman and Sallenger, 1993). A narrow-banded infragravity spectrum could either be due to the input of single frequency from offshore, which seems highly unlikely given the random character of the wave groups, or by resonance of a specific frequency over an existing bar topography (e.g., Kirby et al., 1981). In the latter case, the question remains how the bar was formed earlier.

If there is a single infragravity frequency, linear shore-parallel bars may be generated by infragravity waves without a longshore standing pattern, viz. leaky and single-mode alongshore progressive edge waves (Bowen, 1980).

Morphology with an alongshore rhythmicity, however, requires stationary alongshore variations in drift velocity. The most simple case then consists of two edge waves of the same frequency, modal number and amplitude, but travelling in opposite direction, resulting in a perfect alongshore standing wave pattern. Bowen and Inman (1971) showed that the residual flow caused by this pattern resulted in the formation of a crescentic bar with a length equal to half the longshore edge-wave length. Holman and Bowen (1982) extended Bowen and Inman's work to show that any combination of different edge wave modes of the same frequency could result in a complex alongshore rhythmic morphology, provided that these different modes would possess a phase coupling. Significant phase coupling is conceivable when a beach is located between well-defined reflectors such as headlands or groynes. However, on an uninterrupted beach, like along major parts of the Dutch coast, it is hard to imagine.

The best location to look for the presence of resonantly enhanced infragravity frequencies is the swash on the beach, because all standing infragravity waves have an antinode in surface elevation here. In a swash energy spectrum significant peaks are expected in case of resonantly enhanced modes. However, most infragravity swash spectra measured on the beach of barred systems are white (e.g., Holman and Sallenger, 1993; Ruessink et al., 1998a), indicating that bars do not tend to select specific infragravity frequencies. This casts significant doubt on the causality between nearshore bars and standing infragravity waves.

Further doubt arises from the morphological behaviour predicted by standing-wave models. They predict all bars in a multiple bar system to be generated at the same time. This seems to be at odd with the observed decadal bar behaviour at the Dutch coast. In the cyclic pattern, the outer bar is a remnant of a bar that was once generated in the inner nearshore and migrated to its outer nearshore position. In other words, the outer bar was not formed in the outer nearshore zone. Moreover, the presumed resonance over a pre-existing bar topography is a stabilising factor on the bar position, which contrasts with the systematic long-term cyclic behaviour. The systematic movement of the bars would therefore imply a systematic, cyclic change in the standing-wave characteristics on the same time scale as the bar cycle; however, this seems highly unlikely given the broadbanded nature of the incoming infragravity waves and the constant statistics of the wave climate over the duration of the bar cycle.

On the whole, support for the standing-wave hypothesis on natural uninterrupted beaches is meagre. Most field experiments fail to show a single dominant infragravity frequency, while the presence of such an enhanced frequency is imperative for the hypothesis. Moreover, the predicted fixation of the morphology and the absence of a cyclic offshore forcing are in contrast to

the observed cyclic behaviour of nearshore bars along the Dutch coast. As such, the standing-wave hypothesis is not further considered here.

Type 2a: first-order infragravity motions

O'Hare and Huntley (1994) investigated whether the formation of nearshore bars could be coupled to the (first-order) orbital infragravity motion instead of to the (second-order) drift velocities. They assumed that sediment is stirred by short waves on a wave group time scale and is subsequently transported by the orbital infragravity motion. A fixed phase relation between the stirring (i.e., the short-wave envelope) and the low-frequency orbital motion causes a net sediment transport. Moreover, if the phase coupling varies systematically over the profile, a pattern of erosion and sedimentation areas emerges, resulting in bar and trough formation. O'Hare and Huntley assumed their model to be more successful in bar generation than those based on the drift velocity patterns for the following three reasons:

- the orbital motion does not require time to become a stable feature of the hydrodynamics,
- the first-order motion is approximately uniform in the vertical and, therefore, the dependence of the location of bar formation on the type of sediment transport vanishes and
- the second-order drift velocities are presumably an order of magnitude smaller than the first-order orbital motions.

O'Hare and Huntley (1994) demonstrated that the coupling between short-wave stirring and transport due to monochromatic infragravity orbital motion may indeed result in positions with sediment convergence and divergence (and thus in bar formation).

O'Hare (1994) extended O'Hare and Huntley's (1994) work and examined the effect of random wave groups and of the relative strength of bound and breakpoint-forced long waves on bar formation. O'Hare (1994) still observed a systematic pattern of divergence and convergence when he used the same parameter setting as in O'Hare and Huntley (1994), but with random wave groups. This pattern is mainly caused by the dominance of the breakpoint-forced long wave in the entire infragravity-wave field. An increase in the height of the incident bound long wave results in a destruction of the convergence-divergence pattern, even if the wave groups are monochromatic. A dominance of bound waves in the infragravity flow field would therefore inhibit bar formation. Thus, besides the bandwidth of the incident long-wave motion, the relative strength of bound and breakpoint-forced long waves seems to be critical for bar formation as well.

Summarising O'Hare's work, bars may be generated even by irregular wave groups if breakpoint-forced long waves prevail, whereas a dominance of bound

long-wave motion tends to inhibit bar formation. The existing literature (e.g., Abdelrahman and Thornton, 1987; Roelvink and Stive, 1989; Ruessink et al., 1998b) points to the dominance of bound long waves in the infragravity-induced sediment transport, which indicates that the bar generation mechanism proposed by O'Hare may not be valid under natural conditions, at least, under those observed along the Dutch coast.

Type 2b: first-order infragravity motions (or, an extended breakpoint hypothesis)

The second subclass of bar-generating models involving primary infragravity motions consists of flows that play a dominant role in the surf zone. Its development has a long history. The first flow to be recognised was the mean offshore directed current under breaking waves (undertow), transporting sand stirred by short-wave orbital motion in a seaward direction (for instance, Dyhr-Nielsen and Sørensen, 1970; Stive and Battjes, 1984; Dally, 1987). Outside the surf zone the undertow vanishes and the sand is deposited, resulting in bar formation just seaward of the breaker point. If the waves reform, a multiple bar system can develop (Dyhr-Nielsen and Sørensen, 1970). The model was extended by the inclusion of wave asymmetry (Stive, 1986), generally moving sand in the onshore direction, especially outside the surf zone. Clearly, the combination of undertow and wave asymmetry results in accumulation of sand just outside the surf zone. Accordingly, this bar formation mechanism has often been referred to as the 'breakpoint-hypothesis'. A further refinement was made by Roelvink and Stive (1989), who included the wave grouping-induced long-wave flow. This flow may result in a non-zero transport in case of a systematic coupling between short-wave stirring and long-wave orbital motion, as noted in the previous subsection. This is, for example, the case for group-bound long waves, which generally results in a seaward directed transport because of the concurrence of the bound-wave trough and the enhanced stirring during the higher waves in a group (Larsen, 1982). Roelvink and Stive (1989) found all three flows to be of roughly equal magnitude during their laboratory experiments. They subsequently derived model formulations for all three flow components (i.e. undertow, short-wave velocity asymmetry and group-forced infragravity orbital motions). Exclusion of one of the flows from their model still resulted in bar formation, but with bar characteristics, such as distance from the shoreline and height, different from their laboratory observations. Roelvink and Stive (1989) could not establish whether their laboratory findings were representative of other situations, like natural beaches. Recent field measurements, which strongly suggest that the three flows identified in this subsection are indeed responsible for interannual morphological change, are presented in the next section.

3 Infragravity waves and nearshore morphology: recent observations

Recent measurements of instantaneous near-bed hydrodynamics and sediment concentrations in the multiple bar system of Terschelling (the Netherlands; Figure 2) have confirmed that sediment is transported on a range of time scales, namely the short-wave scale, the infragravity group scale and the time (hour) averaged scale (Ruessink et al., 1998b). As an example, Figures 3a-c present values of the high-frequency, low-frequency and mean sediment flux, respectively, measured at a (nominal) height of 0.15 m above the bed in 5.5 m depth at the seaward side of the outer bar (labelled as P2 in Figure 2). Positive (negative) values indicate onshore (offshore) directed fluxes. The values are
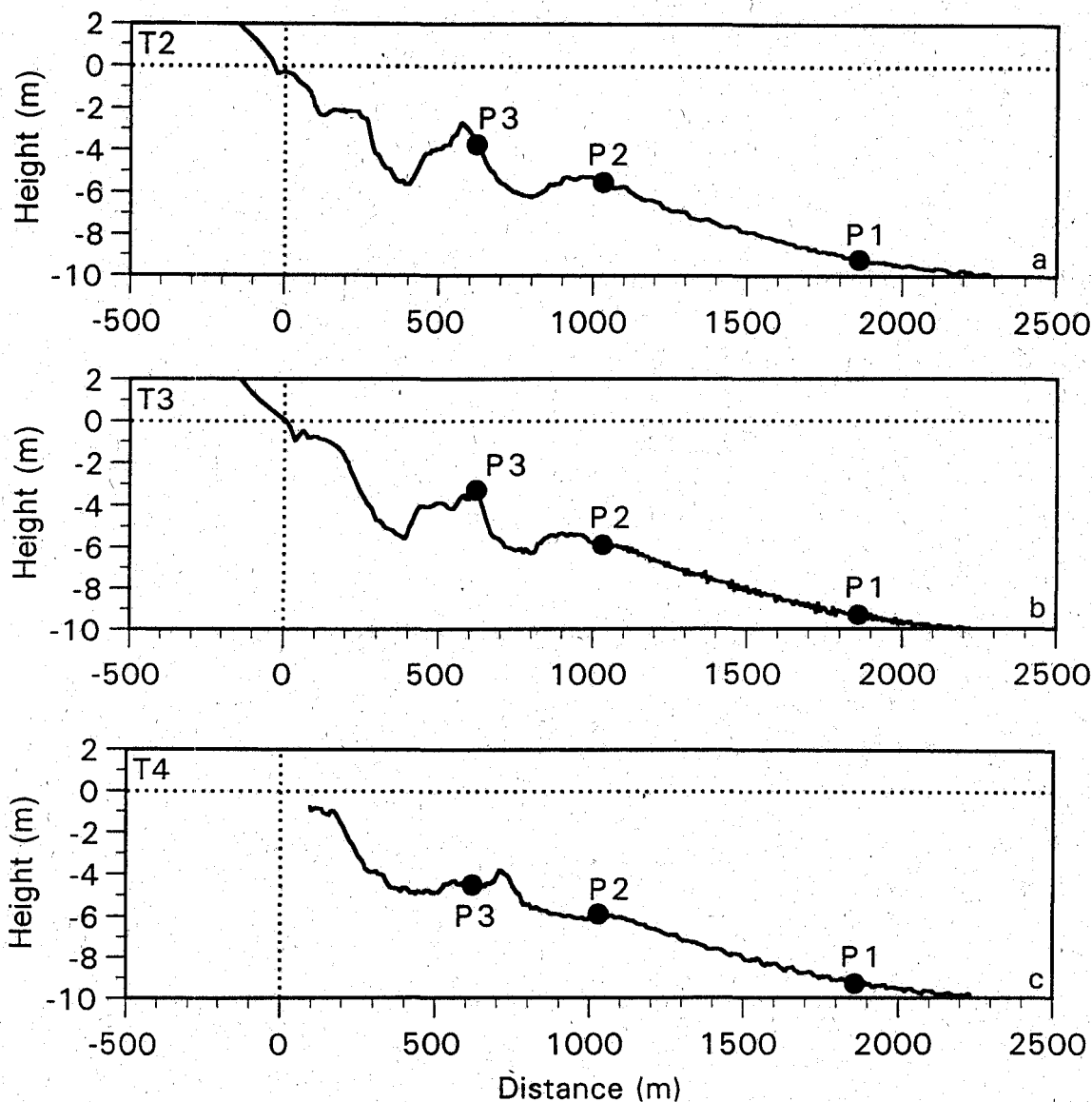
Figure 2   *Cross-shore profile of the measurement section at the onset of the a) T2-campaign, b) T3-campaign and c) T4-campaign. Height is with respect to NAP (= Dutch ordnance level; 0 m NAP is about Mean Sea Level).*

plotted as a function of the relative wave height, defined as the local ratio of the short-wave significant wave height H_s to the water depth h. H_s/h values in excess of 0.33 indicate breaking conditions. As can be seen, non-zero fluxes were only observed for $H_s/h > 0.3 - 0.35$, i.e. conditions during which P2 experienced breaking waves. The high-frequency fluxes (Figure 3a) were onshore directed, related to wave asymmetry in the horizontal plane, and at a first glance of approximately equal magnitude to the mean fluxes, which were of opposite sign (Figure 3c). The mean flows under breaking conditions were offshore directed and generally increased with H_s/h. This strongly suggests that these flows were undertows (Ruessink et al., 1998b). The low-frequency fluxes were offshore directed as well, but were considerably smaller than the other fluxes. Frequency-domain analysis of the available time series showed a 180-degree phase shift between the low-frequency orbital motion and the low-frequency (i.e., group enhanced) component of the instantaneous sediment concentration, consistent with bound-wave mechanism explained previously. The high-frequency and mean flux increased rapidly with H_s/h, while the infragravity flux remained about constant. The sum of the three fluxes, the net flux, was still offshore directed (Figure 3d), but of smaller magnitude than the mean flux. This demonstrates that the cross-shore sediment transport at this position (at least, at the height above the bed shown here) is a delicate balance between contributions by mean flows and by short and long waves. Comparable results were obtained at P3 (Ruessink et al., 1998b).

It has to be kept in mind that the conclusions that can be drawn from Figure 3 only apply to the sensor height above the bed. They are not necessarily representative of the depth-averaged suspended load. In addition, the measurements did not provide any knowledge of the bedload. At present, this part of the total load cannot be measured successfully in the field. For these reasons, Ruessink et al. (1998b) turned to sediment transport modelling. In this approach they adopted Bailard's (1981) energetics method, in which the bedload and the depth-averaged suspended load related to the various mechanisms are computed as a linear sum of moments of the near-bed flow. The bedload and suspended load transport rate, q_b and q_s, respectively, are then assumed to be proportional to (cf. Roelvink and Stive, 1989; Ruessink et al., 1998b)

$$\langle q_b \rangle \propto \langle |u_h|^2 u_h \rangle + 3\langle |u_h|^2 u_l \rangle + 3\bar{u}\langle |u_h|^2 \rangle \qquad (1a)$$

and

$$\langle q_s \rangle \propto \langle |u_h|^3 u_h \rangle + 4\langle |u_h|^3 u_l \rangle + 4\bar{u}\langle |u_h|^3 \rangle \qquad (1b)$$
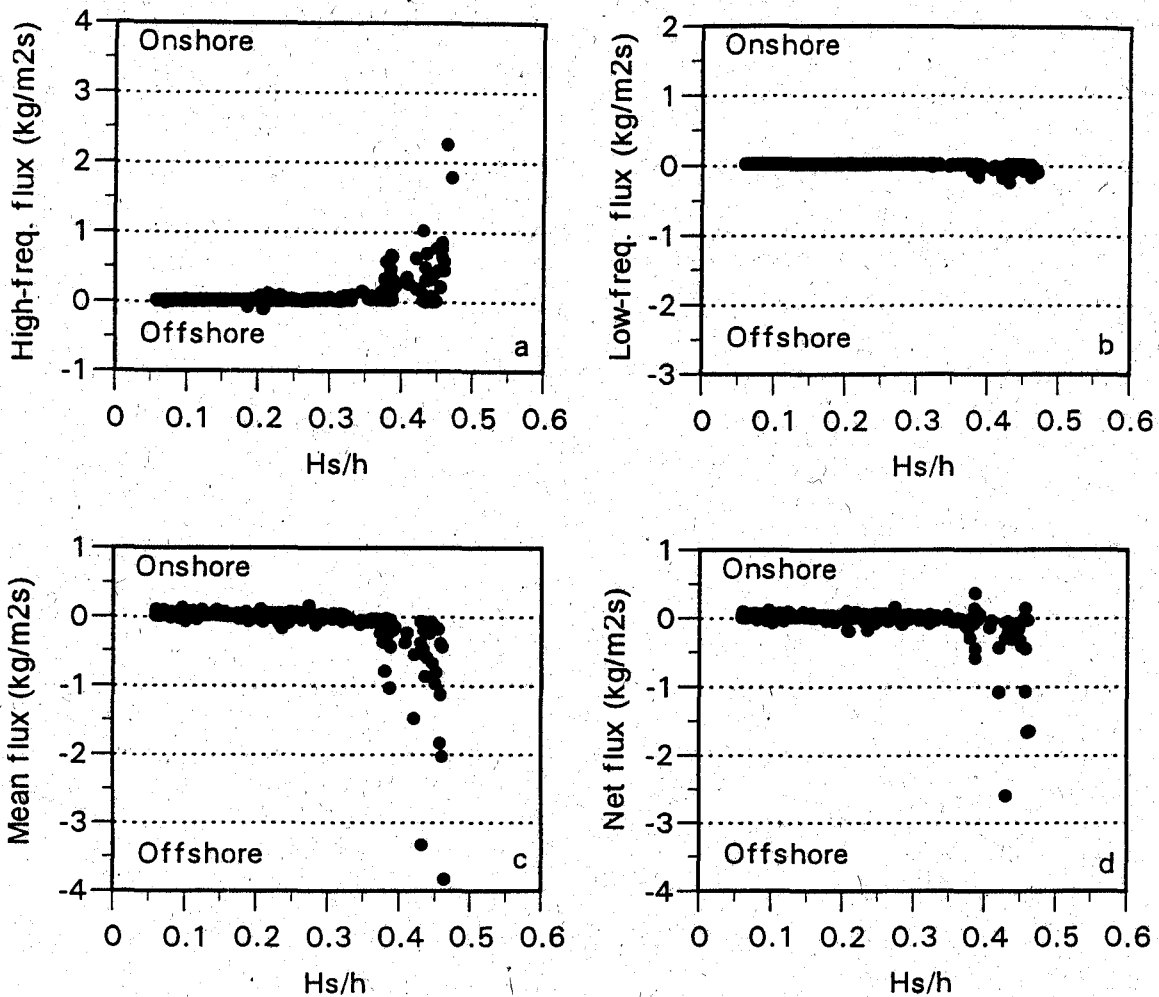
Figure 3 *Measured a) high-frequency, b) low-frequency, c) mean and d) net fluxes at $z =$ 0.15 m as a function of the local relative wave height H_s/h at P2 (T4-campaign).*

in which u_h and u_l are the instantaneous cross-shore high-frequency and low-frequency orbital flow, $\bar{u}$ is the cross-shore mean flow and the angle brackets indicate time-averaging. As can be deduced from Equation (1), the stirring of sand is proportional to u_h to the power of two in the bedload and three in the suspended load. The three terms on the right-hand-side of Equations (1a) and (1b) are hereafter referred as the high-frequency, low-frequency and mean-flow velocity moments, respectively. The high-frequency moments are non-zero when the stirring terms $|u_h|^2$ and $|u_h|^3$ are systematically related to u_h. This is the case for short-wave asymmetry about the horizontal plane ('skewness'), caused by non-linearities. It results, in general, in positive ('onshore direction') values. The low-frequency moments attain a non-zero value if the predicted sediment stirring is systematically coupled to u_l. Such a coupling exists, as discussed above, in case of group-bound long waves, which results in a negative ('offshore direction') values as the phase shift between the wave envelope and the forced infragravity motions amounts to approximately 180 degrees. The

mean-flow moments correspond to the advective transport by a mean cross-shore flow. Clearly, the direction of this part of the total load equals that of the flow, which under breaking conditions is seaward because of the wave-driven undertow. The adopted energetics approach is, at least qualitatively, consistent with the transport mechanisms observed in Figure 3. An extensive account of the velocity moment in Equations (1a) and (1b) at P1, P2 and P3 can be found in Ruessink et al. (1998b). These authors computed the moments with measured time series of instantaneous velocity, obtained at 0.25 m above the bed. As the bedload moments were predicted to be smaller than the suspended load moments by an order of magnitude, they were discarded from further analysis.

In Figures 4a-c the calculated suspended load moments at P2 are plotted versus the local relative wave height. Their sum, the net velocity moment, is shown in Figure 4d. In these plots, the moments are binned corresponding to $H_s/h \pm 0.01$. The vertical lines around the class-mean values (black dots) are the standard deviations in each H_s/h class. The high-frequency terms showed characteristic positive values and increased rapidly with H_s/h (Figure 4a). The infragravity-induced moments were, as expected, negative, related to the systematic concurrence of high values of $|u_h|^3$ and bound long-wave troughs. At P2 they remained about constant with increasing H_s/h for $H_s/h > 0.33$ (Figure 4b). Obviously, the total oscillating (i.e., sum of high- and low-frequency) suspended transport rate was onshore directed. The average mean-flow terms indicated onshore and offshore transports of a very small magnitude for situations with H_s/h values less than 0.33 (Figure 4c). Apparently, the cross-shore mean flow under non-breaking conditions was very small and did not result in a dominant transport direction. In contrast, the mean moments had negative (offshore) values when P2 experienced surf zone conditions, related to the wave-driven undertow. In general, the mean-flow moment was of comparable magnitude to the high-frequency term. Thus, despite the increase in breaking intensity with H_s/h, the growth in the mean-flow moment was counteracted by an about equal rise in the short-wave oscillatory term. In other words, under breaking conditions the amount of sand transported offshore by the undertow was opposed by an approximately equal amount moved onshore by the wave asymmetry. Clearly, the depth-averaged suspended transport is a delicate balance between two large components of equal magnitude, but of opposite sign. From this viewpoint, even a systematic contribution of a small velocity moment, such as related to forced infragravity waves (Figure 4b), may not be neglected. The fact that the average value of the net moment was generally close to that of the low-frequency term (e.g., compare Figures 4b and d) substantiates this further. Comparable results were obtained for the remaining instrumented positions (Ruessink et al., 1998b).
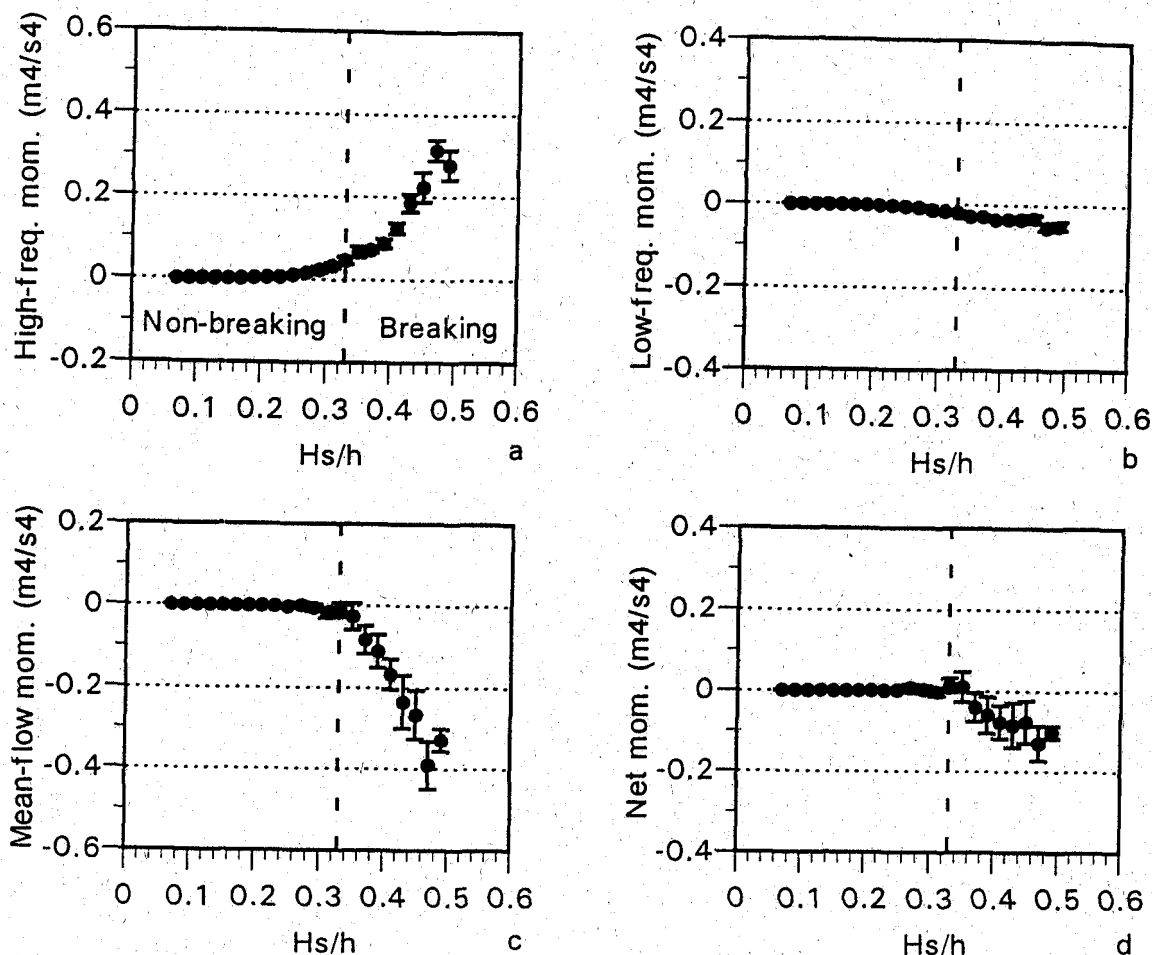
Figure 4   The magnitude of: a) the high-frequency, b) the low-frequency, c) the mean-flow and d) the net fourth-order velocity moments at P2 as a function of the local relative wave height Hs/h. The vertical line through each class-mean value is the standard deviation. The vertical dashed line in each plot marks the onset of breaking (H$_s$/h = 0.33).

Summarising, both the direct observations presented in Figure 3 and the model computations in Figure 4 indicate that short waves, bound infragravity waves and cross-shore mean flow are likely to be the relevant small-scale processes that may ultimately be responsible for medium-scale cyclic bar behaviour. This will be further discussed in the next section.

4   Discussion

Various approaches may be adopted to enhance the understanding of medium-scale bar behaviour using the underlying small-scale processes as starting point. One of these is the running of a deterministic profile model for a long time span. An example is presented by Roelvink et al. (1995). With the deterministic

cross-shore profile model UNIBEST-TC the authors could reproduce the 15 year bar cycle at Terschelling (Netherlands) with reasonable accuracy. However, various new concepts, like breaking delay and a drastic change in the bottom slope effect, had to be included to obtain stable medium-scale results. These concepts have, however, not been sufficiently tested against field measurements. Furthermore, the Terschelling model settings did not appear to function properly in a later test case at another barred site (Reniers and Roelvink, 1996). Thus, it is not a priori clear that small-scale process-based models are yet the most suitable tools for explaining medium-scale bar behaviour (see also De Vriend, 1997). The model description of small-scale processes (waves, currents, sediment transport) involves various assumptions and simplifications, which lead to inherent inaccuracies. It further appears that model validation against small-scale field and laboratory data still reveals remarkable differences between observed and predicted morphological changes (e.g., Nairn and Southgate, 1993; Schoonees and Theron, 1995). Therefore, it can be doubted whether the running of small-scale deterministic profile models over larger time scales will produce reliable results. Other problems associated with the deterministic modelling approach may be the prohibitive computer run time and the possible build-up of numerical errors (De Vriend, 1997).

Another approach is based on direct field observations of small-scale processes. Such observations allow to investigate which small-scale processes may be of importance in the long run, as shown in the previous section, and which conditions dominate medium-scale transports, provided, of course, that the field measurements are conducted during a sufficiently long time period to include all relevant conditions. An additional advantage is that estimates of sediment transport rates can be computed from measured near-bed hydrodynamics and are no longer hampered by the inaccuracy of hydrodynamic model predictions.

The observational method has proved to be quite successful in hindcasting observed small-scale bar development (e.g., Gallagher et al., 1998); its application to medium-scale cyclic bar behaviour is, however, still in its infancy. A first promising step has recently been taken by Ruessink and Terwindt (1998). They proposed a conceptual model that qualitatively explains the cyclic behaviour of multiple bar systems based on an analysis of the Terschelling (NOURTEC) field observations. These measurements comprised of a 15 week data set of near-bed hydrodynamics at three cross-shore positions (Figure 2) and were conducted under a wide range of hydrodynamic conditions. The statistics of the offshore wave conditions and water levels of this data set were virtually identical to the medium-scale statistics. Thus, these observations are considered to be representative of the time scale of the cyclic bar behaviour.

The proposed model can be seen as a first step to a more coherent morphodynamic model for medium-scale multiple-bar behaviour.

Essential to Ruessink and Terwindt's conceptual model is the probabilistic analysis of the available field data at P1, P2 and P3. For each site, it involved the coupling of computed sediment transport rates, q, categorised into groups of H_s/h, to the discrete medium-scale distribution function of H_s/h, $p(H_s/h)$. As the adopted approach involves transport magnitudes and frequency-of-occurrence, it is also referred to as the frequency-magnitude approach. $p(H_s/h)$ was computed by dividing the H_s/h range from 0 to 0.6 into equal intervals with a width of 0.02. The proportion $s(H_s/h)_j$ that the jth H_s/h class contributes to the total medium-scale sediment transport rate $<q_{ms}>$ was computed as

$$s(H_s/h)_j = \frac{p(H_s/h)_j . q(H_s/h)_j}{\langle q_{ms} \rangle} \qquad (2)$$

in which $q(H_s/h)_j$ is the sediment transport rate in the jth H_s/h class and $<q_{ms}>$ is given by

$$\langle q_{ms} \rangle = \sum_{j=1}^{n} p(H_s/h)_j . q(H_s/h)_j \qquad (3)$$

n equals the number of classes (= 30 here). It are the H_s/h binned suspended load velocity moments that Ruessink and Terwindt (1998) used as estimates of $q(H_s/h)_j$ in Equation (2). Frequency-magnitude relationships were thus calculated separately for the suspended load by the incident sea-swell, the infragravity waves and the cross-shore mean flow at P1, P2 and P3. The subscripts h, l and mf are added below to indicate the medium-scale transport rates by these three transport mechanisms.

The measured H_s/h classified velocity moments at P1, P2 and P3 are shown in the left column of Figure 5. The observed discrete distribution functions of H_s/h are plotted in the second column of Figure 5. The third and fourth column in Figure 5 present the relative and cumulative contributions of the H_s/h classes to the medium-scale transport rates of the various processes, respectively. In the computations of the frequency-magnitude relationships, the medium-scale transport by bound infragravity waves, $<q_{ms}>_l$, was used as denominator in Equation (2) at each site. Thus, the cumulative value of $s(H_s/h)_j$ over all n H_s/h classes equals 1 for the infragravity-induced transport. The corresponding cumulative values for the short waves and the cross-shore mean
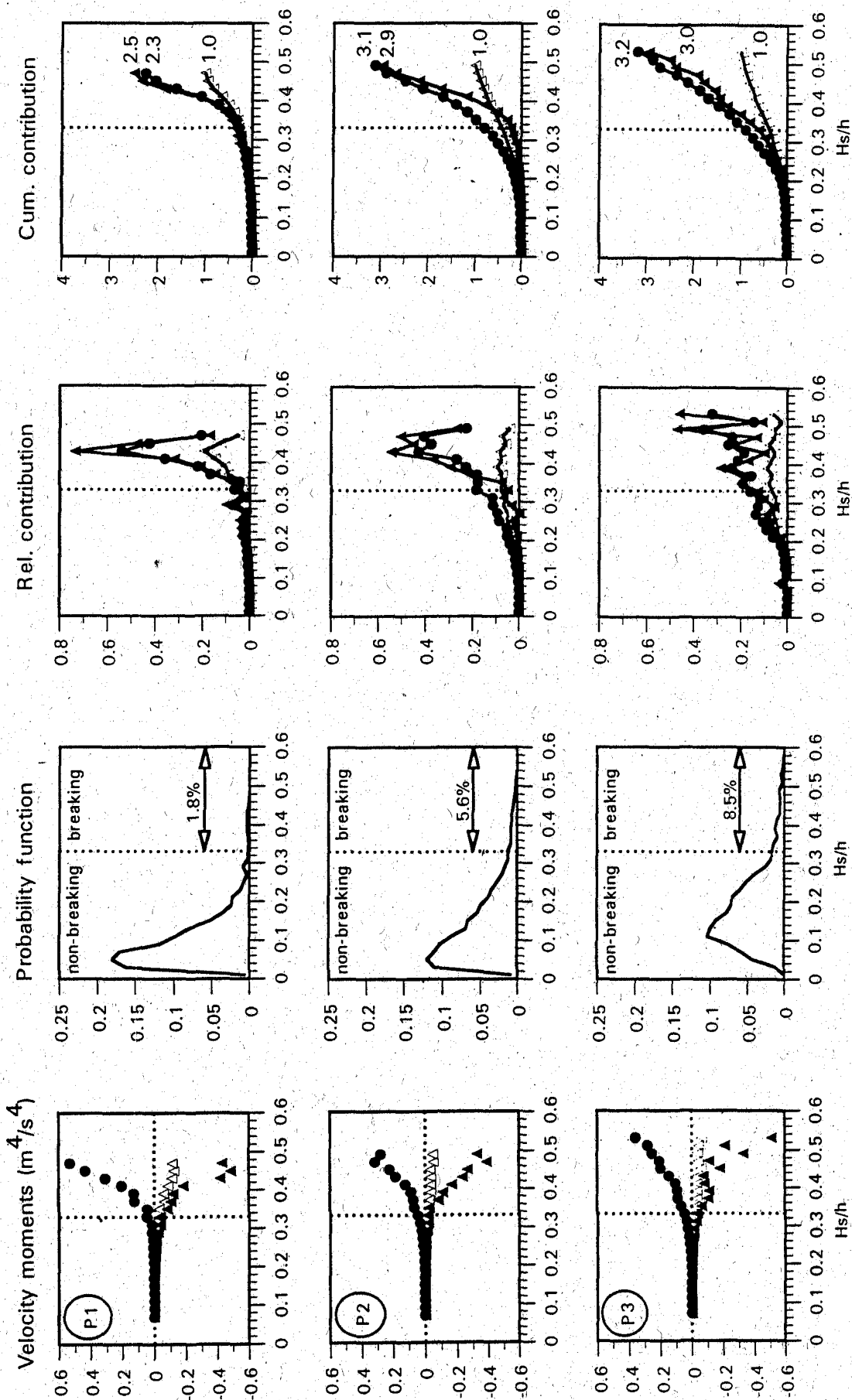
218

Velocity moments (m⁴/s⁴) — Probability function — Rel. contribution — Cum. contribution

flow equal the relative size of $<q_{ms}>_h$ and $<q_{ms}>_{mf}$ with respect to $<q_{ms}>_l$. For instance, the value of 2.5 at P1 (upper graph in fourth column) implies that at P1 = 2.5 $<q_{ms}>_l$.

As can be seen in Figure 5, the medium-scale sediment transport rate by short waves was of approximately equal magnitude to that by the mean flow. Both were about three times as large as that induced by the infragravity waves. At P1 (9-m depth) breaking conditions were by far the most dominant situations, despite the fact that breaking occurred for only 1.8% in time (Figure 5). Classes with $(H_s/h)_i \geq 0.33$ contributed to over 90% of $<q_{ms}>_h$ and $<q_{ms}>_{mf}$. In more shallow water (3 - 5 m; P2 and P3) non-breaking conditions became increasingly important for $<q_{ms}>_h$ ($\approx$ 30%), whereas $<q_{ms}>_{mf}$ remained entirely restricted to surf zone conditions ($\approx$ 90%). If these findings are extrapolated to more shallow water, they develop into a pattern that describes 'summer' and 'winter' transport directions (cf. Winant et al., 1975; Komar, 1998). This means a predominately onshore transport driven by short waves under prolonged non- or weakly breaking conditions and a prevailing offshore transport under surf zone conditions.

On the whole, the adopted frequency-magnitude approach and the aforementioned extrapolation suggest that the H_s/h events that are most effective from the standpoint of contribution to the medium-scale sediment transport in the onshore direction change from predominantly surf zone conditions ($H_s/h > 0.33$) just beyond the outer bar zone towards predominately non-breaking conditions ($H_s/h < 0.33$) on the beach. In contrast, the conditions most effective for the annual offshore directed transport remain restricted to situations with $H_s/h = 0.33$. In other words, there is a gradual cross-shore change from a delicate hourly balance of opposing transport directions (where hourly implies within the same H_s/h class) seaward of the outer bar zone towards a predominantly seasonal balance (i.e. non-breaking versus breaking time periods) on the beach. This suggestion
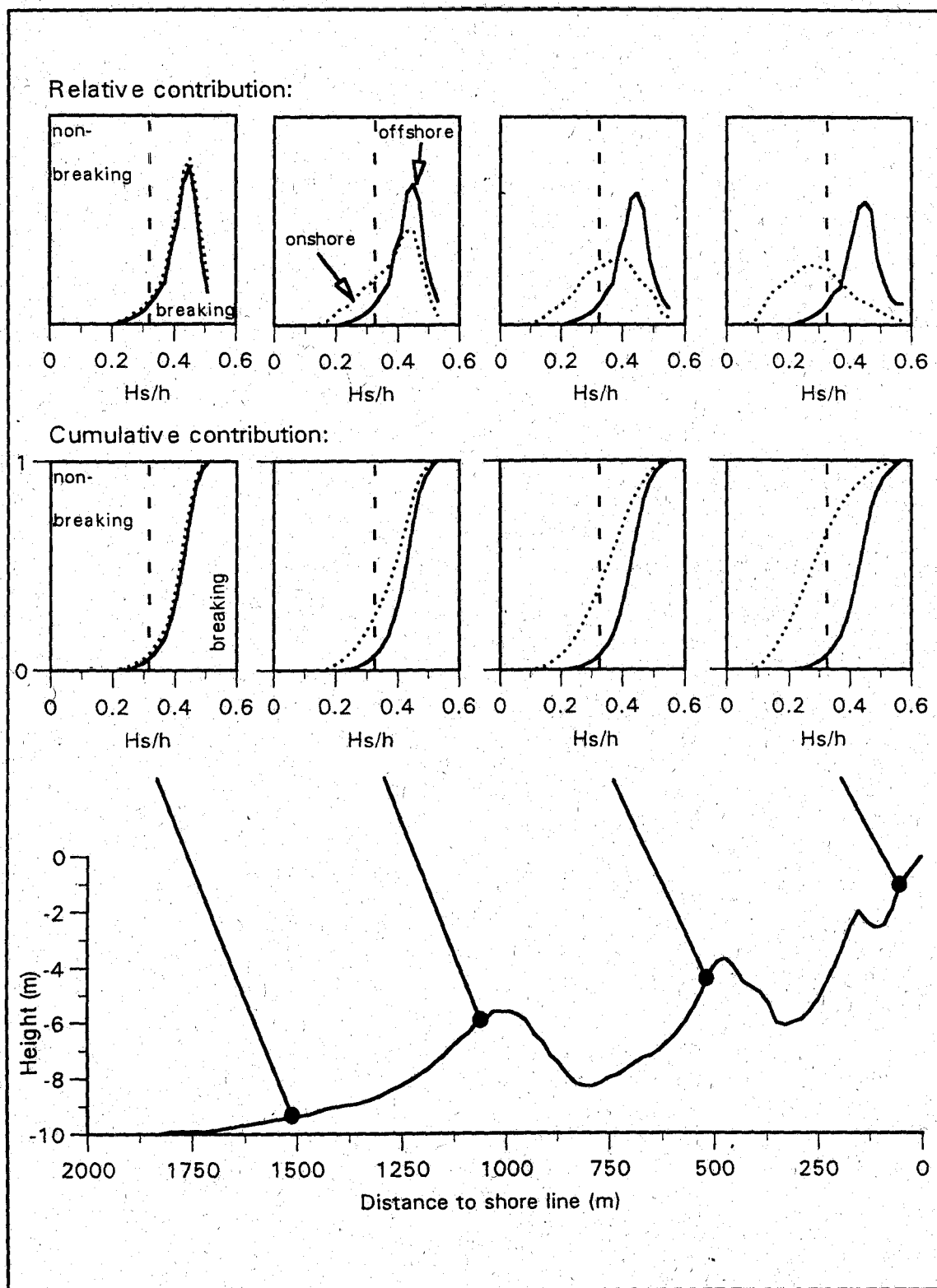
Figure 6   *Schematic diagram showing the cross-shore change from an hourly to seasonal*
balance of onshore and offshore sediment transport rates. The cumulative value
of the contribution of all H_s/h classes has been set to 1 for each process at every
position. For simplicity, the sediment transport rates are described in 'onshore'
and 'offshore' directions. See text for further explanation.

is illustrated in a very schematic way in Figure 6, in which $<q_{ms}>_1$ is neglected and the high-frequency and mean-flow subscripts are replaced by onshore (on) and offshore (off), respectively. As can be seen, the nearshore bar zone is an intermediate area: non-breaking conditions do contribute to $<q_{ms}>_{on}$, but they are of smaller medium-scale importance than on the beach. In contrast, $<q_{ms}>_{off}$ is dominated by breaking conditions over the entire cross-shore profile.

The observed gradual cross-shore change in the small-scale driving conditions is one of the key elements in Ruessink and Terwindt's (1998) conceptual model. The reader is referred to their paper or to Ruessink (1998) for a full description of the conceptual model, including morphological examples and further underlying assumptions and considerations. The model can be briefly summarised as follows. When a bar shifts in the seaward direction (stage 2), it is located in deeper water. Here, the importance of onshore directed transport under non-breaking conditions is less than at its original position. Consequently, the bar cannot return to its former position near the beach. In stage 2 the yearly sediment transport directed offshore is hypothesised to be larger than that directed onshore: the bar moves in a seaward direction. However, the more the bar shifts further seaward, the more is the offshore directed transport under surf zone conditions going to be opposed by the simultaneously existing onshore transport. At the end, there is an hourly balance, and the offshore bar migration stops. The outer bar may disappear under weakly breaking conditions; the decay is associated with an onshore directed sediment transport (cf. Wijnberg, 1995). In nature, bar stages 2 and 3 actually coincide: sediment converges at the seaward side of the bar in stage 2, which implies that, as observed by Ruessink and Kroon (1994), this bar grows in volume with distance offshore. Model calculations suggested that the lowering of the outer bar in stage 3 results in a shift to higher values in the frequency of occurrence of the relative wave height in the inner bar zone. This may cause the yearly offshore directed transport to grow in size with respect to the onshore directed transport: the decay of the outer bar safeguards the bar cycle by causing a new bar to move offshore.

221

5   Summary and conclusions

This paper has addressed the linkage between infragravity waves and nearshore bars. Early work mainly focussed on second-order drift velocities associated with cross-shore standing waves. Although realistic looking bar morphology can be produced, the inherent assumptions are often not met under natural conditions. Furthermore, the predicted medium-scale bar behaviour strongly

contrast with our phenomenological knowledge that this behaviour has a cyclic nature. More recently, it has been recognised that primary infragravity (orbital) motions interact with other surf zone flows, such as wave asymmetry and undertow. Field observations suggest that the role of infragravity waves is of only minor importance (e.g., Figure 5). The subsequent explanation of medium-scale cyclic bar behaviour by the underlying small-scale transport mechanisms is still new and is as yet only formulated in a qualitative conceptual way. It is hoped that the conceptual model proposed by Ruessink and Terwindt (1998) is a first step to a more coherent morphodynamic model for medium-scale cyclic bar behaviour.

Acknowledgements

References

Abdelrahman, S.M. and E.B. Thornton, 1987. Changes in the short wave amplitude and wavenumber due to the presence of infragravity waves. Proc. Coastal Hydrodynamics, ASCE, 458-478.

Bailard, J.A., 1981. An energetics total load sediment transport model for a plane sloping beach. Journal of Geophysical Research, 86, 10938-10954.

Bowen, A.J., 1980. Simple models of nearshore sedimentation: beach profiles and longshore bars. In: The coastline of Canada, edited by S.B. McCann, pp. 1-11.

Bowen, A.J. and D.I. Inman, 1971. Edge waves and crescentic bars. Journal of Geophysical Research, 76, 8662-8671.

Carter, T.G., P.L.-F. Liu and C.C. Mei, 1973. Mass transport by waves and offshore sand bedforms. Journal of Waterways, Harbors and Coastal Engineering Division, ASCE, 165-184.

Dally, W.R., 1987. Longshore bar formation - surf beat or undertow? Proc. Coastal Sediments'87, ASCE New York, 71-86.

De Vriend, H.J., 1997. Prediction of aggregated-scale coastal evolution. Proc. Coastal Dynamics'97, ASCE, New York, 644-653.

Dyhr-Nielsen, M. and T. Sørensen, 1970. Some sand transport phenomena on coasts with bars. Proc. of the 12th Int. Conf. on Coastal Eng., ASCE, 855-866.

Gallagher, E.L., S. Elgar and R.T. Guza, 1998. Observations of sand bar evolution on a natural beach. Journal of Geophysical Research, 103, 3203-3215.

Holman, R.A. and A.J. Bowen, 1982. Bars, bumps and holes: models for the generation of complex beach topography. Journal of Geophysical Research, 87, 457-468.

Holman, R.A. and A.H. Sallenger, 1993. Sand bar generation: a discussion of the Duck experiment series. Journal of Coastal Research, SI 15, 76-92.

Kirby, J.T., R.A. Dalrymple and P.L.-F. Liu, 1981. Modification of edge waves by barred-beach topography. Coastal Engineering, 5, 35-49.

Komar, P.D., 1998. Beach processes and sedimentation. Second Edition. Prentice Hall, New Jersey (USA), 544 pp.

Larsen, L.H., 1982. A new mechanism for seaward dispersion of midshelf sediments. Sedimentology, 29, 279-283.

Lippmann, T.C., R.A. Holman and K.K. Hathaway, 1993. Episodic, nonstationary behavior of a double bar system at Duck, North Carolina, USA, 1986-1991. Journal of Coastal Research, SI 15, 49-75.

Nairn, R.B. and H.N. Southgate, 1993. Deterministic profile modelling of nearshore processes. Part 2. Sediment transport and beach profile development. Coastal Engineering, 19, 57-96.

O'Hare, T.J., 1994. The role of long waves in sand bar formation - a model exploration. Proc. Coastal Dynamics'94, ASCE New York, 74-88.

O'Hare, T.J. and D.A. Huntley, 1994. Bar formation due to wave groups and associated long waves. Marine Geology, 116, 313-325.

Reniers, A. and J.A. ROELVINK, 1996. Diagnostic studies NOURTEC. Comparison between Torsminde and Terschelling nourishment. Report on model investigation (concept). Delft Hydraulics Report H1698, 13 pp.

Roelvink, J.A. and M.J.F. Stive, 1989. Bar-generating cross-shore flow mechanisms on a beach. Journal of Geophysical Researh, 94, 4785-4800.

Roelvink, J.A., Th. J.G.P. Meijer, K. Houwman, R. Bakker and R. Spanhoff, 1995. Field validation and application of a coastal profile model. Proc. Coastal Dynamics'95, ASCE New York, 818-828.

Ruessink, B.G., 1998. Infragravity waves in a dissipative multiple bar system. PhD Thesis, Utrecht University, the Netherlands, 245 pp.

Ruessink, B.G. and A. Kroon, 1994. The behaviour of a multiple bar system in the nearshore zone of Terschelling, the Netherlands: 1965-1993. Marine Geology, 121, 187-197.

Ruessink, B.G. and J.H.J. Terwindt, 1998. The behaviour of nearshore bars on the time scale of years: a conceptual model. Submitted to Marine Geology.

Ruessink, B.G., M.G. Kleinhans and P.G.L. van den Beukel, 1998a. Observations of swash under highly dissipative conditions. Journal of Geophysical Research, 103, 3111-3118.

Ruessink, B.G., K.T. Houwman and P. Hoekstra, 1998b. The systematic contribution of transporting mechanisms to the cross-shore sediment transport in water depths of 3 to 9 m. Marine Geology, 152, 295-324.

Schoonees, J.S. and A.K. Theron, 1995. Evaluation of 10 cross-shore sediment transport/morphological models. Coastal Engineering, 25, 1-41.

Shand, R.D. and D.G. Bailay, 1998. A review of net offshore bar migration with photographic illustrations from Wanganui, New Zealand. Journal of Coastal Research, in press.

Stive, M.J.F., 1986. A model for cross-shore sediment transport. Proc. of the 20th Int. Conf. on Coastal Eng., ASCE New York, 1550-1564.

Stive, M.J.F. and J.A. Battjes, 1984. A model for offshore sediment transport. Proc. of the 19th Int. Conf. on Coastal Eng., ASCE New York, 1962-1974.

Winant, C.D., D.L. Inman and C.E. Nordstrom, 1975. Description of seasonal beach changes using empirical eigenfunctions. Journal of Geophysical Research, 80, 1979-1986.

Wijnberg, K.M., 1995, Morphologic behaviour of a barred coast over a period of decades. PhD Thesis, Utrecht University, the Netherlands, 245 pp.

Wijnberg, K.M. and J.H.J. Terwindt, 1995. Quantification of decadal morphological behaviour of the central Dutch coast. Marine Geology, 126, 301-330.